Electronic Supplementary Information

$Ca_3Al_2B_8O_{18}$: Borate with Graphene-like Layer Featuring Two Types of Topological Six-Membered Rings Induced by [AlO_4] Unit

Ziting Yan[a,b], Dongdong Chu[a,b], Zhihua Yang [a,b], Shilie Pan*[a,b] and Min Zhang*[a,b]

[a]Research Center for Crystal Materials; State Key Laboratory of Functional Materials and Devices for Special Environmental Conditions; Xinjiang Key Laboratory of Functional Crystal Materials; Xinjiang Technical Institute of Physics and Chemistry, Chinese Academy of Sciences, 40-1 South Beijing Road, Urumqi 830011, China.

[b]Center of Materials Science and Optoelectronics Engineering, University of Chinese Academy of Sciences, Beijing 100049, China.

*Corresponding authors: E-mails: slpan@ms.xjb.ac.cn, zhangmin@ms.xjb.ac.cn.

Experimental section

Reagents.

$Ca(NO_2)_2$ (MAKLIN, 92-94 %), AlF_3 (MAKLIN, 99 %), Al_2O_3 (Aladdin, 99.99 %), B_2O_3 (Aladdin, 99.99 %) were used as the starting materials without further treatment.

Syntheses.

Single crystals of $Ca_3Al_2B_8O_{18}$ (CABO) were prepared through conventional high-temperature solution methods in an open environment. The mixture of $Ca(NO_2)_2$, AlF_3, and B_2O_3 at ratios of 2:2:3 was ground completely and transferred to a platinum crucible. Next, the crucible was put into a programmable temperature electric furnace and heated to 850 °C with a rate of 60 °C h^{-1}, kept at this temperature for 12 hours. Thereafter, the crucible was decreased to 650 °C at the speed of 2.4 °C h^{-1}, lowered to 450 °C with a rate of 4.8 °C h^{-1}, and then further cooled to ambient temperature at a rate of 24 °C h^{-1}. The final colorless crystals of CABO could be mechanically separated from the reaction systems and selected using a microscope.

The polycrystalline samples of CABO were obtained via the solid-state reaction techniques. $Ca(NO_2)_2$, Al_2O_3, and B_2O_3 were mixed and ground evenly with a stoichiometric ratio, and loaded into a ceramic crucible. To decompose the nitrite, the mixed sample was preheated and held at about 700 °C for 12 h first. Subsequently, it was thoroughly ground, gradually raised to 830 °C, and held at this temperature for 72 h with several intermediate grindings and mixings. The pure phase of CABO was obtained and confirmed through powder X-ray diffraction (PXRD) conducted at room temperature.

Single-Crystal X-ray Diffraction.

A transparent CABO crystal with a regular shape was chosen for structure determination. Single-crystal XRD data were collected on a Bruker D8 Venture diffractometer using graphite-monochromated Mo Kα radiation (λ = 0.71073 Å) and integrated with the SAINT program.[1] The structure was resolved using the direct method, and the structure was optimized by full-matrix least-squares techniques using the program suite SHELXTL on F^2. The single-crystal data were handled with OLEX2 software,[2] and the related compounds were examined by PLATON for higher symmetry.[3]

Powder X-ray Diffraction.

On a Bruker D2 PHASER X-ray diffractometer equipped with graphite monochromatic Cu Kα radiation (λ = 1.5418 Å, 296 K), powder XRD patterns were

characterized. The scanning angle range (2θ) for the test was from 5 to 70 ° and the scan step width and rate were 0.02 ° and 1 s/step, respectively.

Thermal Analysis.

The thermal gravimetric (TG) and differential scanning calorimetry (DSC) analyses were carried out on a simultaneous NETZSCH STA 449C thermal analyzer instrument. The sample was encased in the Pt crucible and heated from ambient temperature to 800 °C at a rate of 5 °C·min^{-1} under a continuous flow of nitrogen gas.

Elemental Analysis.

To ascertain the elements in CABO, the energy dispersive X-ray spectroscopy (EDS) was conducted using a SUPRA55VP field emission scanning electron microscope fitted with a BRUKER X-ray Flash-SDD-5010 energy-dispersive X-ray spectrometer.

Infrared Spectroscopy.

To favorably verify the structural units, the infrared (IR) spectroscopy was recorded in the wavelength range of 400−4000 cm^{-1} at room temperature using a Shimadzu IR Affinity-1 Fourier transform infrared (FT-IR) spectrometer. Dried KBr was used as the reference and samples were mixed evenly with it in a weight ratio of 1: 100.

UV−vis−NIR Diffuse Reflectance Spectrum.

To determine the accurate absorption edge of CABO, the UV-vis-NIR diffuse reflectance spectrum was characterized under an atmosphere using a Shimadzu SolidSpec-3700DUV spectrophotometer ranging from 200 to 1600 nm with a scan step width of 2 nm.

Theoretical Calculation.

The CASTEP[4] code based on density generalized theory serves as a powerful tool to unravel the electronic and energy band structures of CABO, and the electronic structures of the reported series were investigated using density functional theory (DFT). The exchange-correlation potential was treated by the Perdew–Burke–Ernzerhof (PBE) method in the generalized gradient approximation (GGA)[5] and interactions between the ionic cores and electrons were described by norm-conserving pseudopotential (NCP). The subsequent orbital electrons were considered as valence electrons: Ca-4s^2, Al-3$s^2$3p^1, B-2$s^2$2p^1, O-2$s^2$2p^4. The cut-off energy was fixed at 780 eV, and the Monkhorst-Pack k-point meshes were chosen to span less than 0.04 Å^{-1} in the Brillouin zone to ensure the calculated results were sufficiently accurate.[6] The other

calculation parameters and convergent criteria were set by the default values of the CASTEP code. The birefringence of CABO was calculated based on the dielectric function $\varepsilon(\omega) = \varepsilon_1(\omega) + i\varepsilon_2(\omega)$.[7] The imaginary part $\varepsilon_2(\omega)$ of the dielectric function can be determined from the electronic structures, while the real component $\varepsilon_1(\omega)$ can be acquired through the Kramers-Kronig transformation. Consequently, the refractive indices and the birefringence (Δn) can be calculated.

$$\zeta = \sum_g [N_c Z_a \Delta\rho^b]_g / (n_1 E_o)$$

Polycrystalline powder samples of CABO were prepared through the solid-state reaction techniques for further characterization. The XRD patterns of the samples are mostly in agreement with the theoretical one, but unfortunately, there are small amounts of $Al_4B_2O_9$ impurity that could not be removed (Figure S4). The thermal analysis was recorded to determine the thermal behaviors of CABO, the TG and DSC curves are shown in Figure S5. There is an evident endothermic peak at around 855 °C on the heating DSC curve, and the TG curve has no obvious weight loss, indicating that CABO is stable up to 855 °C. To further investigate its melting behaviors, the as-prepared polycrystalline powder was placed into a platinum crucible heated to 900 °C until melted, and then cooled very slowly to room temperature. The PXRD pattern of the melted sample exhibits a difference from that of the initial sample, indicating that CABO may melt congruently. The introduction of additional flux is required to realize the crystal growth.

Table S1. Crystal data and structure refinement for $Ca_3Al_2B_8O_{18}$.

Empirical formula	$Ca_3Al_2B_8O_{18}$
Formula weight	548.68
Temperature	297.0 K
Crystal system, space group	monoclinic, $P2_1/n$
Unit cell dimensions	a = 9.146(3) Å b = 8.067(2) Å, β= 90.903(10)° c = 18.527(5) Å
Volume	1366.9(7) Å^3
Z, Calculated density	4, 2.666 g/cm^3
Absorption coefficient	1.453 mm^{-1}
F (000)	1080.0
Crystal size	0.251 × 0.090× 0.073 mm
Theta range for data collection	4.936 to 50.052°
Limiting indices	-10 ≤ h ≤ 10 -9 ≤ k ≤ 9 -22 ≤ l ≤ 20
Reflections collected / unique	9230 / 2405 [R(int) = 0.0996]
Completeness to theta	100 %
Absorption correction	Numerical
Refinement method	Full-matrix least-squares on F^2
Data / restraints / parameters	2405 / 0 / 284
Goodness-of-fit on F^2	1.069
Final R indices [I>2$sigma$(I)] [a]	R_1 = 0.0647, wR_2 = 0.1487
R indices (all data) [a]	R_1 = 0.0925, wR_2 = 0.1707
Largest diff. peak and hole	0.86 and -0.72 e.Å^{-3}

[a] $R_1 = \sum||F_o|-|F_c||/\sum|F_o|$ and $wR_2 = [\sum w(F_o^2 - F_c^2)^2/\sum wF_o^4]^{1/2}$ for $F_o^2 > 2\sigma(F_o^2)$.

Table S2. Atomic coordinates ($\times 10^3$) and equivalent isotropic displacement parameters ($Å^2 \times 10^3$) for $Ca_3Al_2B_8O_{18}$. U(eq) is defined as one third of the trace of the orthogonalized U_{ij} tensor.

Atom	x	y	z	U(eq)	BVS
Ca(1)	1552.8(16)	4598.5(19)	2495.7(8)	17.7(4)	2.240
Ca(2)	5000	5000	5000	24.3(6)	2.087
Ca(3)	0	0	5000	41.7(8)	2.165
Ca(4)	-922.6(16)	10114(2)	2409.0(9)	20.0(4)	1.898
Al(1)	3590(2)	1726(3)	6199.4(13)	18.9(6)	2.782
Al(2)	1278(2)	6892(3)	6375.2(13)	18.5(6)	2.894
B(1)	6100(9)	1446(11)	3360(5)	17.7(18)	3.069
B(2)	3770(9)	3085(11)	3594(5)	15.5(17)	3.042
B(3)	1449(9)	1426(11)	3480(5)	17.6(19)	3.075
B(4)	3597(9)	5802(2)	5082(3)	17.0(18)	3.017
B(5)	2707(9)	1849(11)	4764(5)	17.7(18)	3.038
B(6)	1816(9)	7074(12)	3585(3)	21(2)	3.049
B(7)	1329(9)	8059(10)	3508(5)	17.0(18)	3.015
B(8)	-1156(10)	6602(11)	3253(5)	19.8(19)	2.981
O(1)	5460(5)	-42(6)	3425(3)	20.7(12)	1.993
O(2)	7568(6)	1571(7)	3256(3)	22.2(12)	2.010
O(3)	5335(5)	2917(6)	3372(3)	19.8(12)	2.047
O(4)	2861(5)	1913(6)	3200(3)	17.9(12)	2.099
O(5)	3328(5)	4763(6)	3401(3)	18.6(12)	2.080
O(6)	5198(5)	6580(6)	3812(3)	20.8(12)	1.794
O(7)	3803(6)	2795(7)	4386(3)	21.6(12)	2.041
O(8)	2705(6)	1353(7)	5374(3)	25.3(13)	1.904
O(9)	1512(5)	1416(7)	4262(3)	19.3(12)	2.220
O(10)	314(5)	2522(6)	3193(3)	19.0(12)	1.979
O(11)	2823(5)	7623(6)	3369(3)	18.8(12)	2.024
O(12)	310(5)	6785(6)	3161(3)	20.4(12)	1.961
O(13)	-1776(6)	5054(7)	3296(3)	22.4(13)	1.968
O(14)	-2103(5)	7940(7)	3224(3)	21.8(12)	1.857
O(15)	1038(5)	9714(6)	3204(3)	16.7(11)	2.003
O(16)	987(6)	7990(7)	4280(3)	21.3(12)	2.134
O(17)	1395(6)	7116(7)	5456(3)	25.7(13)	1.944
O(18)	3041(6)	6266(7)	4535(3)	23.6(13)	2.165

Table S3. Selected bond lengths [Å] and angles [deg] for $Ca_3Al_2B_8O_{18}$.

B(1)-O(1)	1.342(10)	Al(1)-O(6)#3	1.760(6)
B(1)-O(2)	1.363(10)	Al(1)-O(8)	1.745(6)
B(1)-O(3)	1.378(10)	Al(1)-O(14)#6	1.764(6)
B(2)-O(4)	1.448(9)	Al(2)-O(2)#3	1.759(6)
B(3)-O(4)	1.453(10)	Al(2)-O(10)#6	1.739(5)
B(2)-O(5)	1.456(10)	Al(2)-O(13)#6	1.741(6)
B(4)-O(5)	1.459(9)	Al(2)-O(17)	1.718(6)
B(3)#8-O(15)	1.518(10)	O(1)-B(1)-O(2)	120.7(7)
B(3)-O(8)	1.417(4)	O(1)-B(1)-O(3)	123.1(7)
B(2)-O(7)	1.487(10)	O(2)-B(1)-O(3)	116.1(7)
B(5)-O(7)	1.382(10)	O(3)-B(2)-O(5)	106.8(2)
B(5)-O(8)	1.339(10)	O(4)-B(2)-O(3)	110.2(6)
B(4)-O(11)	1.437(10)	O(4)-B(2)-O(5)	109.2(6)
B(7)-O(11)	1.438(10)	O(4)-B(2)-O(7)	113.4(6)
B(5)-O(10)	1.465(4)	O(5)-B(2)-O(3)	106.2(6)
B(8)-O(13)	1.375(10)	O(5)-B(2)-O(7)	113.0(6)
B(8)-O(14)	1.385(10)	O(9)-B(3)-O(4)	109.7(6)
B(4)-O(18)	1.534(10)	O(9)-B(3)-O(10)	112.6(6)
B(6)-O(16)	1.380(10)	O(9)-B(3)-O(15)#11	109.8(6)
B(6)-O(18)	1.370(10)	O(5)-B(4)-O(6)	107.5(6)
Ca(1)-O(1)#1	2.506(5)	O(5)-B(4)-O(18)	109.4(6)
Ca(1)-O(5)	2.320(5)	O(11)-B(4)-O(5)	108.7(6)
Ca(1)-O(11)#2	2.336(5)	O(11)-B(4)-O(18)	109.5(6)
Ca(1)-O(12)	2.443(5)	O(8)-B(5)-O(7)	123.9(7)
Ca(2)-O(6)#3	2.552(5)	O(8)-B(5)-O(9)	117.0(7)
Ca(2)-O(7)	2.370(5)	O(9)-B(5)-O(7)	119.1(7)
Ca(2)-O(18)#3	2.225(5)	O(17)-B(6)-O(16)	116.4(7)
Ca(3)-O(8)#4	2.782(5)	O(17)-B(6)-O(18)	123.8(7)
Ca(3)-O(9)	2.269(5)	O(18)-B(6)-O(16)	119.8(7)
Ca(3)-O(16)#5	2.294(5)	O(11)-B(7)-O(12)	109.7(6)
Ca(3)-O(17)#6	2.778(6)	O(11)-B(7)-O(15)	108.7(6)
Ca(4)-O(2)#7	2.412(6)	O(15)-B(7)-O(12)	110.2(6)
Ca(4)-O(5)#1	2.842(6)	O(11)-B(7)-O(16)	112.5(6)
Ca(4)-O(10)#8	2.667(5)	O(16)-B(7)-O(12)	104.3(6)
Ca(4)-O(14)#9	3.125(6)	O(12)-B(8)-O(13)	120.9(7)
Ca(4)-O(15)	2.325(5)	O(12)-B(8)-O(14)	121.8(7)
Al(1)-O(1)#10	1.751(5)	O(13)-B(8)-O(14)	116.9(7)

Symmetry transformations used to generate equivalent atoms:
#1) 1/2-X,1/2+Y,1/2-Z; #2) 1/2-X,-1/2+Y,1/2-Z; #3) 1-X,1-Y,1-Z; #4) -X,-Y,1-Z; #5) +X,-1+Y,+Z; #6) -X,1-Y,1-Z; #7) -1+X,1+Y,+Z; #8) +X,1+Y,+Z; #9) -1/2-X,1/2+Y,1/2-Z; #10) 1-X,-Y,1-Z; #11) +X,-1+Y,+Z.

Table S4. Selected layered borates contain different types of six-membered rings.

Type	Compound	Space group	Composition of units	Ref.
3Δ+3T	$SrBe_2B_2O_7$	$P\bar{6}c2$	$3BO_3+3BeO_4$	40
	$CaAl_2(BO_3)_2O$	$R\bar{3}c$	$3BO_3+3AlO_4$	44
	$BaAl(BO_3)F_2$	$P\bar{6}$	$3BO_3+3AlO_3F_2$	49
	$M_3N_3Li_2Al_4B_6O_{20}F$ (M=K, Rb; N = Sr, Ba)	$P\bar{6}c2$	$3BO_3+2AlO_4+LiO_3F$	14, 41, 50
	$Rb_3Al_3B_3O_{10}F$	$P3_1c$	$3BO_3+2AlO_4+AlO_3F$	45
Topological 3Δ+3T	$Cs_2Al_2(B_3O_6)_2O$	$P6_3$	$3B_3O_6+3AlO_4$	51
	$Cs/RbAlB_3O_6F$	$Pna2_1$	$3B_3O_6+3AlO_3F$	52, 53
	CsB_4O_6F	$Pna2_1$	$3B_3O_6+3BO_3F$	23
	$CsKB_8O_{12}F_2$	$P321$	$3B_3O_6+3BO_3F$	10
	$CsRbB_8O_{12}F_2$	$P\bar{6}c2$	$3B_3O_6+3BO_3F$	10
	$NH_4/Na/RbB_4O_6F$	$Pna2_1$	$3BO_3+3B_3O_6F$	37, 46
	$CsBaB_9O_{15}$	Cc	$3B_3O_6+3BO_4$	57
2Δ+4T	$A_2A_3'B_{16}O_{28}$ (A_2=Rb, Cs; A_3'=Ca, Cd)	$C2/c$	$2BO_3+4BO_4$	47,48
	$CaAl_2B_8O_{18}$	$P2_1/n$	$2BO_3+2BO_4+2AlO_4$	
6T	$CaAlB_3O_7$	$Cmma$	$4BO_4+2AlO_6$	54
	$MB_2O_3F_2$ (M = Pb, Sn)	$P3_1m$	$6BO_3F$	55
Topological 6T	$Na_{11}B_{21}O_{36}X_2$(X = Cl, Br)	$C2/c$	$3B_3O_7+3B_3O_8$	56
	$CsBaB_9O_{15}$	Cc	$3B_3O_7+3BO_4$	57
Δ+5T	$CaAl_2B_8O_{18}$	$P2_1/n$	$BO_3+4BO_4+AlO_4$	

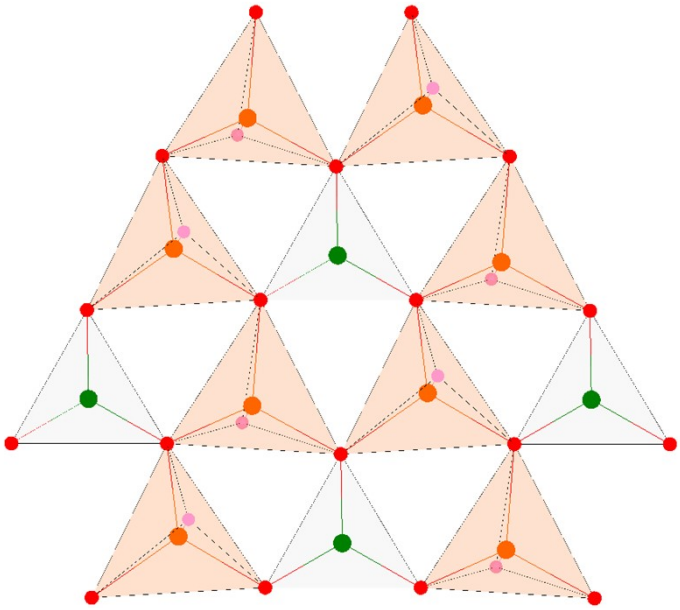

Figure S1. The three membered rings composed of [BO_3] and two [BeO_3F] units in $KBe_2BO_3F_2$.

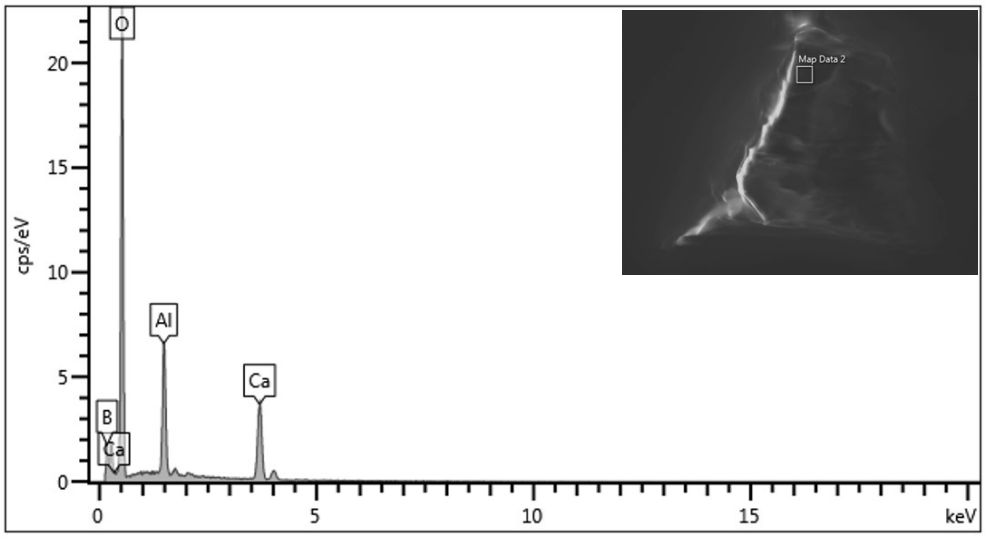

Figure S2. The EDX spectrum of $Ca_3Al_2B_8O_{18}$.

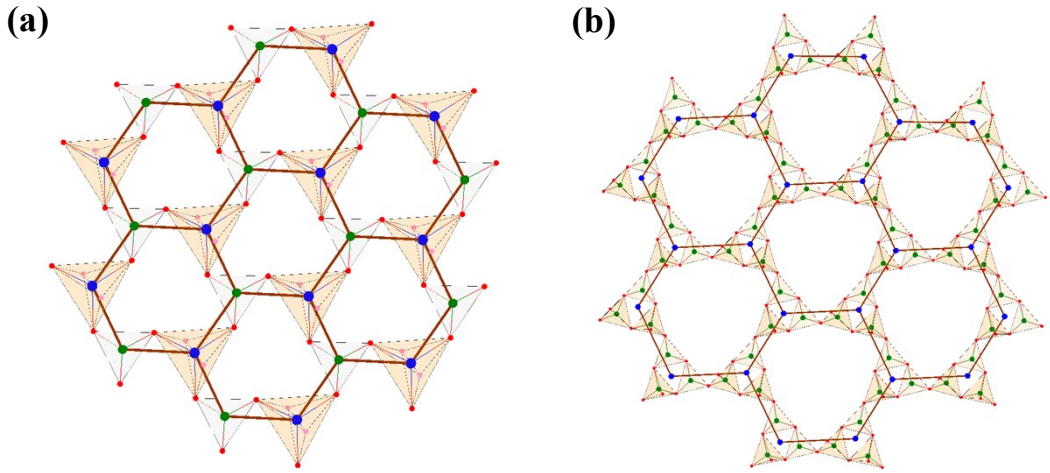

Figure S3. (a) The 3Δ+3T 6-MRs composed of three [BO_3] and three [AlO_3F_2] units in $BaAl(BO_3)F_2$. (b) The 6T 6-MRs composed of three [B_3O_7] and three [B_3O_8] units in $Na_{11}B_{21}O_{36}Cl_2$

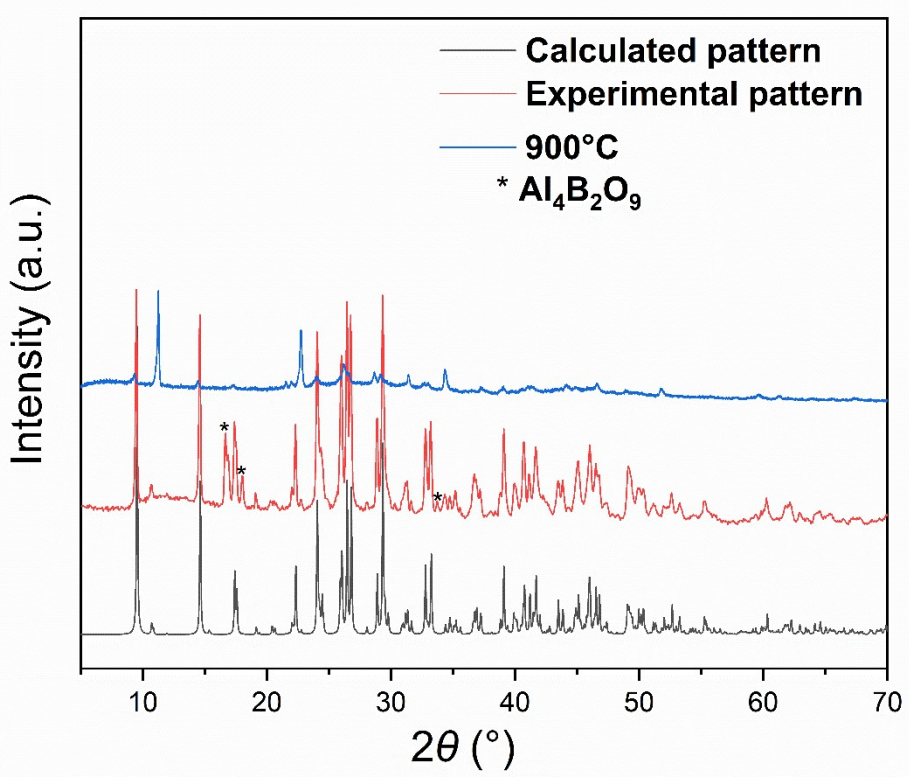

Figure S4. The calculated and experimental powder XRD patterns of $Ca_3Al_2B_8O_{18}$.

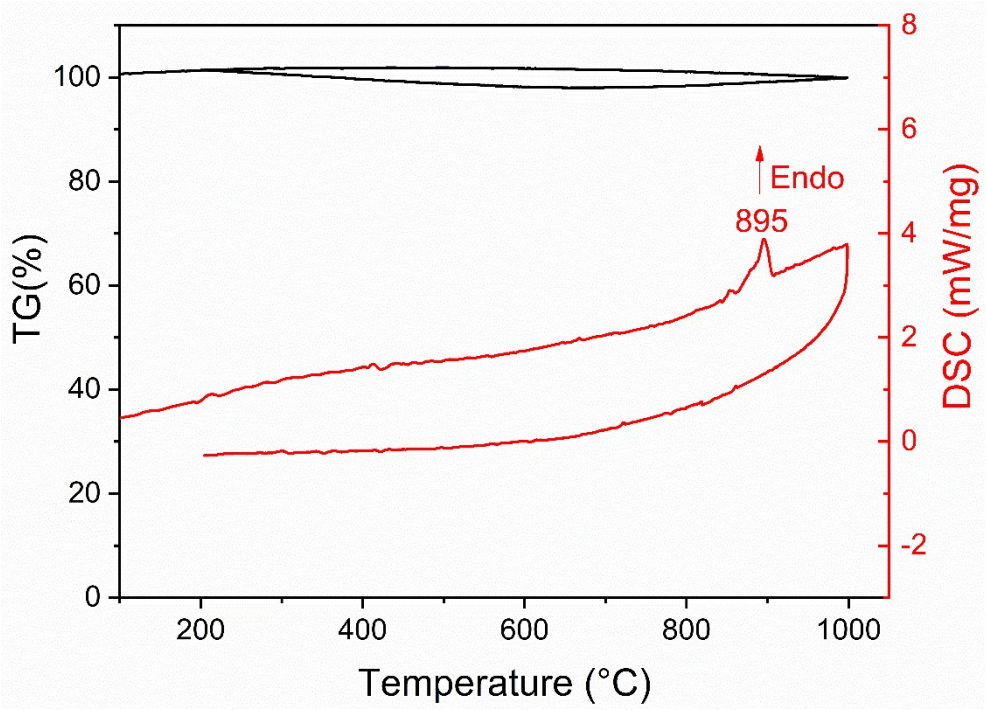

Figure S5. TG and DSC curves of $Ca_3Al_2B_8O_{18}$.

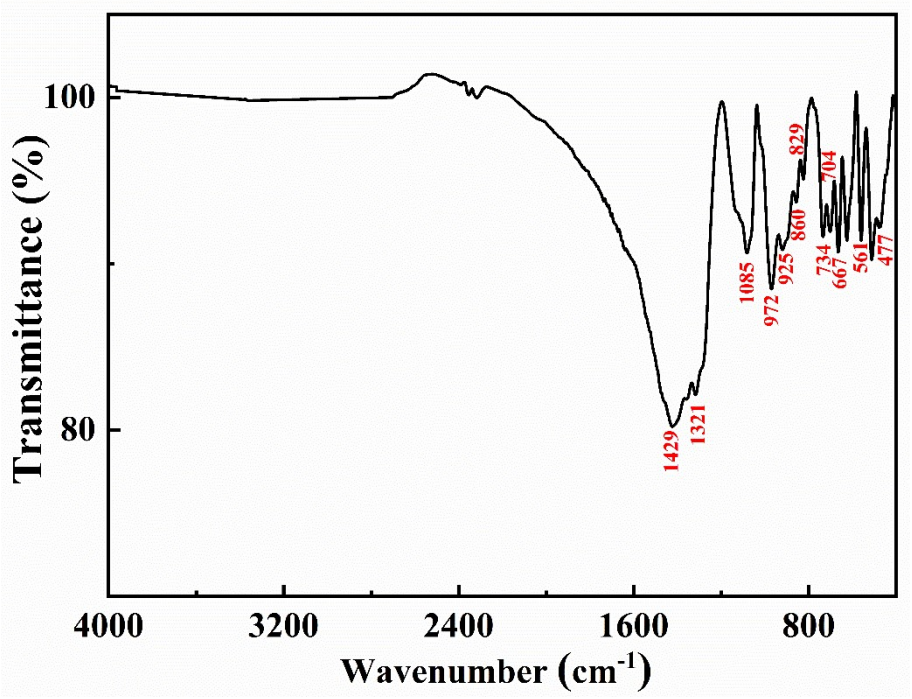

Figure S6. The infrared spectrum for $Ca_3Al_2B_8O_{18}$.

Reference:

1. V. A. SAINT, *Inc., Madison, WI*, 2008.
2. (a) O. V. Dolomanov, L. J. Bourhis, R. J. Gildea, J. A. K. Howard and H. Puschmann, *J. Appl. Crystallogr.*, 2009, **42**, 339-341; (b) G. M. Sheldrick, *Acta Crystallogr. A*, 2008, **64**, 112-122.
3. A. Spek, *J. Appl. Crystallogr.*, 2003, **36**, 7-13.
4. S. J. Clark, M. D. Segall, C. J. Pickard, P. J. Hasnip, M. I. J. Probert, K. Refson and M. C. Payne, *Z. Kristallogr. Cryst. Mater. Lett.*, 2005, **220**, 567-570.
5. (a) L. Kleinman and D. M. Bylander, *Phys. Rev. Lett.*, 1982, **48**, 1425-1428; (b) A. M. Rappe, K. M. Rabe, E. Kaxiras and J. D. Joannopoulos, *Phy. Rev. B*, 1990, **41**, 1227-1230; (c) J. S. Lin, A. Qteish, M. C. Payne and V. Heine, *Phy. Rev. B*, 1993, **47**, 4174.
6. H. J. Monkhorst and J. D. Pack, *Phy. Rev. B*, 1976, **13**, 5188-5192.
7. J. E. Sipe and E. Ghahramani, *Phy. Rev. B*, 1993, **48**, 11705-11722.